

## Superconducting transition-edge sensors in tomorrow physics

C. PEPE

*Istituto Nazionale di Ricerca Metrologica, Dipartimento di Elettronica Telecomunicazioni  
Politecnico di Torino, INFN Sezione di Torino - Torino, Italy*

received 17 February 2023

**Summary.** — Transition-edge sensors (TESs) are outstanding calorimeters based on the steep superconductive transition of a metallic film. Among photon detectors, they belong to the top-tier positions for the high-energy resolutions and the low dark count rates. They are usually applied to detect electromagnetic energy from gamma-ray to visible and submillimetre wavelengths, but their use goes further. INRiM is presently involved in the development of TESs that pertain to different fields. In fact, TES capability of revealing massless or massive particles, while measuring their energies, can be applied in the quantum technologies, metrology and telecommunications, resolving photon signals from noise and counting them, as well as in the astrophysical and particle frameworks, from neutrino mass to multi-messenger astronomy measurements. For all these reasons, TESs are constantly under development in order to fulfil the more severe experimental requirements. The latest results obtained at INRiM on TESs performances and applications will be presented.

### 1. – Introduction

Transition-edge sensors (TESs) are highly sensitive detectors developed in low-temperature physics. TESs work as microcalorimeters and use superconducting thin films to measure changes in temperature caused by absorbed energy [1]. According to Irwin and Hilton [2], TESs are among the detectors with the highest-energy resolution, making them particularly well suited for precision measurements in physics and astronomy. Moreover, they are able to detect single particles across a wide range of energies, from infrared to gamma photons [3-6].

In addition to their high-energy resolution, TESs also have low dark count rate and high quantum efficiency [7, 8], making them well suited to play a crucial role in quantum optics [9] and detecting rare events in particle physics.

In this paper, I will delve into the technology behind TESs detectors and explore their potential applications in both quantum optics and particle physics. I will present new results and techniques developed to improve their performance, and discuss the future

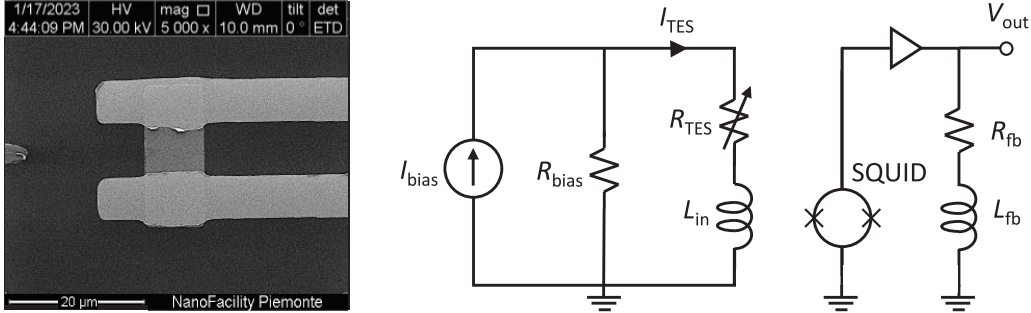


Fig. 1. – Left: scanning electron microscopy image of a  $9 \times 9 \mu\text{m}^2$  TES fabricated with a 30 nm thick aluminum film and 60 nm thick niobium wiring. Right: schematic of the circuit where the TES is voltage-biased if the condition  $R_{TES} \gg R_{bias}$  is met. The current changes in the TES branch are measured through the input coil using a DC-SQUID operated in a flux-locked loop.

prospects of TESs in these fields. I will begin by discussing the Single and Entangled photon sources for QUantum METrology (SEQUME) project [10, 11], which aims to develop new technologies for quantum metrology, quantum communication, and quantum computing. Then, I will focus on the Princeton Tritium Observatory for Light, Early-universe, Massive-neutrino Yield (PTOLEMY) project [12,13], which aims to detect relic neutrinos, followed by the Quantum Haloscope Search (QHaloS) experiment, an upgrade of the MuDHI experiment [14], which aims to search for dark photons in the mass range  $1.5 \text{ eV}/c^2$ .

## 2. – Operating principle of TES and its performance characteristics

The TES operates based on the principle of negative electrothermal feedback (ETF), which occurs when the TES is voltage-biased and the thermal bath temperature is kept below the critical temperature. The electrical circuit containing the TES, represented as a variable resistor, is shown on the right of fig. 1. TES is voltage-biased for  $R_{TES} \gg R_{bias}$ , the bias current is set such that Joule heating keeps the TES within the transition range.

When a particle is absorbed, the film’s temperature rises, causing an increase in resistance and a decrease in current. This, in turn, reduces the power dissipated by the film, leading to a decrease in temperature until a balance is achieved between Joule heating and heat transfer to the substrate and the film then returns to its initial state. The temporary fluctuation in TES current gives rise to a change in the magnetic flux within  $L_{in}$ . This change is detected by a DC-SQUID, similar to the one described in [15]. To achieve accurate readings, the DC-SQUID operates in a flux-locked loop, where a feedback flux is applied to cancel out any changes in the flux from the input coil, thereby maintaining a constant flux in the SQUID. The output of the readout is a signal proportional to the absorbed energy.

For the purpose of this paper, it is important to note that the TES performance can be described by simplified equations of the energy resolution and the recovery time. These equations are derived in detail in sect. 2 of ref. [1]. Additionally, these equations have been recently summarized in [16], where a new simulation tool for TES performance is introduced and can be accessed at [www.tes.inrim.it](http://www.tes.inrim.it). In the following I list the two simplified equations to highlight the areas where there is room for improvement in TES

performance:

$$(1) \quad \Delta E \approx 2\sqrt{2\ln 2} \sqrt{4k_{\text{B}}T_{\text{C}}^2 \frac{C}{\alpha_I} \sqrt{\frac{n}{2}}} \propto T_{\text{C}}^{\frac{3}{2}},$$

$$(2) \quad \tau_{\text{eff}} \approx \frac{n}{\alpha_I} \frac{C}{G} \propto T_{\text{C}}^{-(n-2)}$$

Where  $T_{\text{C}}$ ,  $C$ , and  $G$  represent the critical temperature, heat capacity, and thermal conductance, respectively. The logarithmic sensitivity,  $\alpha_I = \left. \frac{d \ln R}{d \ln T} \right|_{I_{\text{TES}}}$ , measures the steepness of the superconductive transition. The exponent factor  $n$  for the thermal conductance is a value that is typically between 4 and 6 when electron-phonon decoupling dominates.

The critical temperature of a TES is a parameter that can be easily fine-tuned by choosing the appropriate materials and exploiting physical effects such as the proximity effect [17]. From the equations, it is clear that TESs with lower critical temperatures tend to have better energy resolution, while TESs with higher critical temperatures have shorter recovery times. Improving one performance may come at the expense of the other, and striking a balance between the two is important for achieving optimal performance in specific applications. For instance, a TES with a critical temperature below 100 mK is likely to have good energy resolution but may be unavoidably slow. The optimal choice of critical temperature for a given application depends on the specific requirements of that application. In the next sections I will discuss INRiM ongoing efforts to optimize TESs parameters and align them with the desired performance objectives for the three projects mentioned in the ‘‘Introduction’’.

### 3. – Single and entangled photon sources for quantum metrology

The SEQUME project aims to develop bright entangled photon sources and to demonstrate the quantum advantage achievable using high-purity single-photon sources. Moreover, the project aims to develop a European metrology infrastructure for traceable characterisation of these sources. INRiM is involved in the development of two TESs optimized for 930 nm and 1550 nm. The goal for TESs is to reach a detection efficiency greater than 90% and detection rates greater than 2 MHz, while maintaining an energy resolution better than 0.4 eV to guarantee a good photon-number capability.

The main challenge of the project is to increase the repetition rate to more than 2 MHz, meaning an effective time constant of less than 100 ns. Previous studies, such as [18] and [19], have shown promising results towards this goal using TiAu TESs. To further reduce the effective time constant, considering eq. (2), the direction to follow is to increase the  $T_{\text{C}}$  of the film. The  $T_{\text{C}}$  of TiAu TES is upper-limited by titanium’s intrinsic critical temperature under 500 mK. For this reason, the focus is now oriented towards aluminum, which has a critical temperature on the order of 1 K.

Here I present preliminary results obtained on a  $7 \times 7 \mu\text{m}^2$  Al TES. As shown in fig. 2 (left), the transition of the TES was measured with a  $T_{\text{C}}$  of 1047.5 mK. Although the TES’s energy resolution was not sufficient to discriminate single photons, a response was observed, as shown in fig. 2 (right). The figure also displays oscillations, indicating that the TES response is not stable. As reported in [20], stability in TESs is achieved when

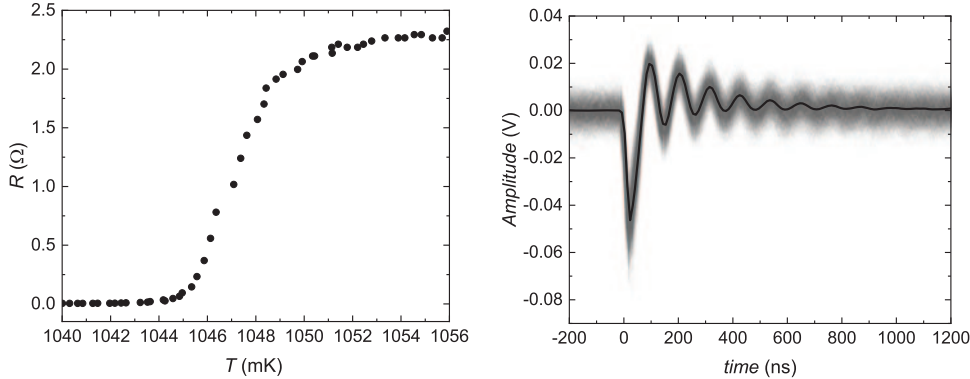


Fig. 2. – Superconductive transition of a  $7 \times 7 \mu\text{m}^2$  Al TES (left). The superposition of 10000 pulses is shown in gray, and the average is shown in black (right). This result was obtained by illuminating the TES with a pulsed monochromatic laser at constant power with emission at 1540 nm, and polarizing the TES at 60% of its normal resistance.

$\frac{\tau_{\text{eff}}}{\tau_{\text{el}}} > 5.8$ , where  $\tau_{\text{el}}$  is the electrical time constant equal to  $L_{\text{in}}/R_{\text{TES}}$ . When the TES was polarized at 60% of its normal resistance,  $\tau_{\text{el}}$  was estimated to be  $\sim 8$  ns. Therefore,  $\tau_{\text{eff}}$  should be less than 50 ns since the condition for stability is not met. However, it is important to maintain stability and improve energy resolution in order to validate this assumption. As such, more effort must be put into enhancing both factors while preserving a fast time response. To improve stability, the electrical time constant,  $\tau_{\text{el}}$ , can be reduced by decreasing the input inductance. To improve energy resolution, the area of the device can be decreased to lower its capacity, and the quality of the film can be improved to enhance the steepness of the transition and increase  $\alpha$ .

In conclusion, the results obtained so far with Al TESs are promising regarding the repetition rate, but more efforts must be put into improving energy resolution and stability. In addition, quantum efficiency is an important issue that will be addressed in sect. 6 of this paper. The INRiM effort towards this goal will be discussed for both the SEQUME and QHalo experiments.

#### 4. – Princeton tritium observatory for light, early-universe, massive-neutrino yield

The goal of the PTOLEMY project is to detect Cosmological Relic Neutrinos, with the objective of obtaining a snapshot of the universe’s first second after the Big Bang [12,13]. This would be accomplished through a  $\beta$ -decay process in a tritium target, where relic neutrinos are identified by observing electron with energies that exceed the  $\beta$ -decay endpoint. In order to differentiate this signal from the  $\beta$ -decay endpoint, the project requires an extremely precise electron detector with an energy resolution of 0.05 eV at 10 eV. Previous studies have demonstrated the high-precision energy measurement capabilities of TES, with a TES fabricated at INRiM exhibiting an energy resolution of 0.11 eV for IR photons [21]. More recent advancements have achieved even better results, such as a  $8 \times 8 \mu\text{m}^2$  TiAu TES that has an energy resolution of 0.067 eV [22]. The INRiM approach towards fulfilling the requirements of the PTOLEMY project is detailed in [23]. In this paper, I present our latest achievements. In comparison to [21,22], TESs with

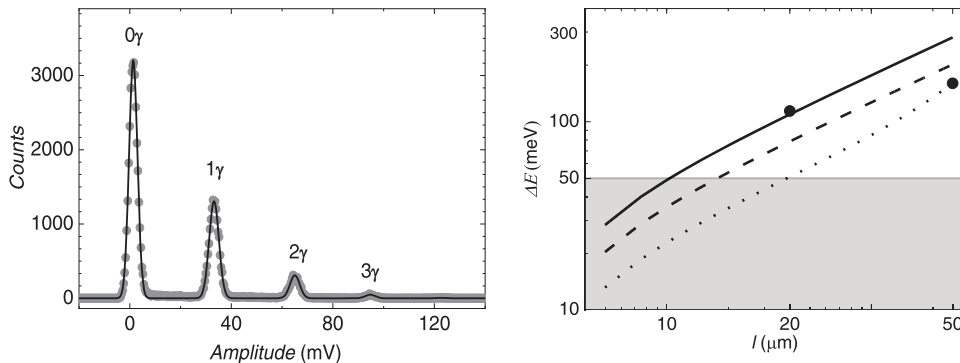


Fig. 3. – Left: histogram of counts for a  $20 \times 20 \mu\text{m}^2$  TiAu TES, energy resolution reached 0.114 eV with 0.8 eV photon. Right: simulation of the energy resolution scaling with respect to length side for 3 critical temperature values, represented by the solid line for 90 mK, the dashed line for 70 mK, and the dotted line for 50 mK. The black circles represent experimental results and the gray area represents the PTOLEMY target.

larger active areas have been explored, resulting in an energy resolution of 0.114 eV for a  $20 \times 20 \mu\text{m}^2$  TiAu TES with a critical temperature of 92 mK as reported in fig. 3 (left). Additionally, this result is represented as a circle in fig. 3 (right) alongside the result from a  $50 \times 50 \mu\text{m}^2$  TiAu TES with a critical temperature of 50 mK. By using the simulation software described in [16], it was possible to model the energy resolution trend as a function of TES dimensions and critical temperature. Our simulation shows that we could achieve an energy resolution of 0.05 eV with a  $20 \times 20 \mu\text{m}^2$  TES with a critical temperature of 50 mK. The next steps will be to realize such a device and demonstrate its ability to reach such high-energy measurement precision. In addition, the collaboration is developing a cryogenic electron gun to demonstrate the TES’s ability to detect low-energy electrons. To fully characterize the detector’s detection efficiency for electrons, experimental measurements are necessary. While the high stopping power of metals suggests near-unit electron detection efficiency, the actual efficiency has yet to be confirmed. Therefore, further experiments are required to determine the detection efficiency of TES for low-energy electrons.

## 5. – Quantum haloscope search

Our best guess is that 85% of the matter in the universe consists of dark matter, some beyond-the-Standard-Model particle that has yet to be discovered. Dark photons, which arise from the extension of the Standard Model, are one of the possible candidates for dark matter. They are a type of dark matter that could be detected through its interaction with ordinary matter through a process known as kinetic mixing [24]. The aim of the QHaloS experiment, which is an upgrade of the MuDHI experiment [14], is to search for dark matter, specifically dark photons, by converting them into standard photons with a stack of alternating dielectric layers. The conservation of momentum prevents a non-relativistic dark photon from converting into a photon, which is inherently relativistic. However, if the medium is altered in such a way that translational invariance is broken, the conversion can happen. This technique for detecting dark photons is known as “dielectric haloscope” and the schematic of the experimental setup is shown in fig. 4.

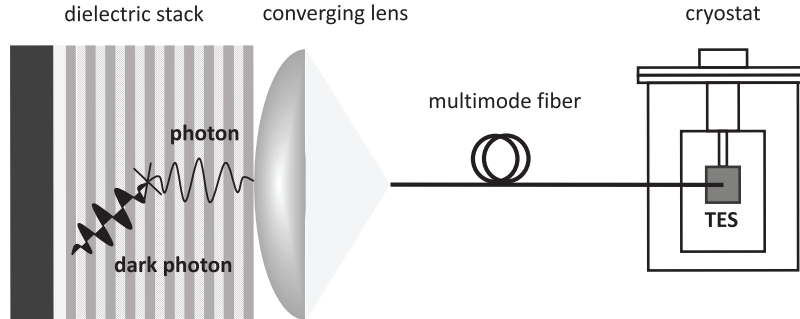


Fig. 4. – Schematic of the QHaloS experiment setup: the stack of dielectric bilayers allows for the conversion of dark photons into ordinary photons. The converted photons are then coupled into a multimode fiber and directed towards the TES.

After a photon has been generated then can be directed to a photosensor, which must be capable of single-photon detection with a high quantum efficiency and low dark count rate. TESs are ideal candidates for this role because they have a low dark count rate and can reach high quantum efficiency, while also being able to provide information on the energy of the absorbed photons.

INRiM TES design has been optimized to meet the specifications of the experiment, such as the detection of 1.5 eV photons with an energy resolution of below 0.2 eV, a detection efficiency above 90%, and an active area sufficient for coupling with a 50  $\mu\text{m}$  diameter core multimode fiber. To achieve these specifications, INRiM aims to develop a TiAu TES with a critical temperature below 100 mK, incorporated into an optical cavity, and covered with an anti-reflection coating. To ensure precise coupling with the multimode fiber, the TES will have a square area of  $60 \times 60 \mu\text{m}^2$ . While this large area is crucial for fiber coupling, it may have a negative impact on the energy resolution. However, INRiM has already achieved impressive results with a  $50 \times 50 \mu\text{m}^2$  TiAu TES with a critical temperature of 50 mK, demonstrating an energy resolution of 0.16 eV at 0.8 eV as shown in fig. 3 (right). In the next section, I will discuss the methods we aim to implement to increase the detection efficiency above 90%.

In conclusion, the QHaloS experiment with TES represents a significant step forward in the search for dark photons, enabling exploration of a previously untapped parameter space, and what makes it even more valuable is that it can be carried out in a lab-scale environment.

## 6. – Detection efficiency

In this section, I will discuss the detection efficiency of TESs for NIR photons.

In this energy range the TES metallic film, whether single or multilayer, serves both as an absorber and detector. The detection process in these cases entails direct heating of the metallic film's electrons, with the absorbed energy rapidly distributed to the entire electron gas, much faster than it would be to the phonon system. TES directly measures the temperature increase of the electron gas after absorption, and the excess heat in the electron gas is eventually released to the phonon system and the substrate serving as a heat sink.

The detection of IR photons with bare TES poses two major challenges. The first

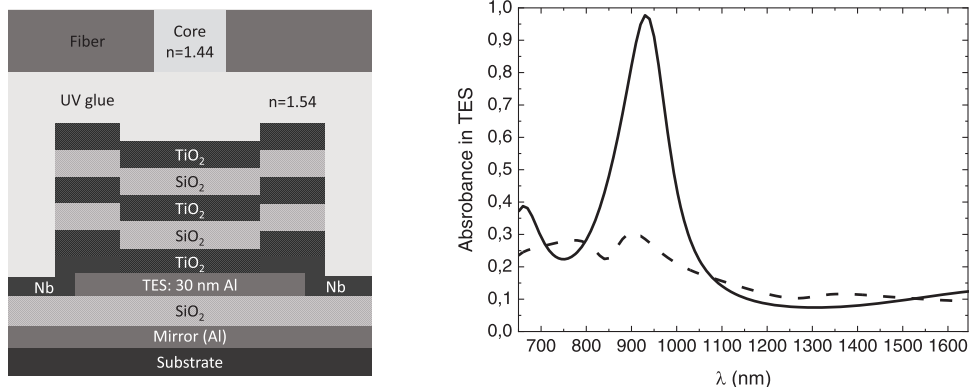


Fig. 5. – Left: schematic of the TES optical cavity and fiber alignment. Right: simulation of TES absorbance with the solid line representing an Al TES in place with optimized thickness of the dielectric layers for maximum absorbance at 930 nm. The dashed line shows the absorbance for a bare TES.

challenge is reflection-induced loss, which must be addressed in the SEQUME project with aluminum reflection at 930 nm and 1540 nm, and in the QHaloS experiment with reflection from the titanium-gold bilayer at 808 nm. The second challenge is transmission loss, which occurs due to the thin thickness of TES and results in a non-zero probability for photons to pass through the material without absorption. A possible solution to these challenges is to embed the TES in an optical cavity and coat it with an anti-reflection material [25]. As shown in [7], this technique can result in an outstanding detection efficiency of 98% at 850 nm with a Ti TES. Figure 5 on the left shows an example of the INRiM design for SEQUME TES. It features a thick layer of Al acting as a mirror, followed by a layer of SiO<sub>2</sub> as a spacer. The TES is then fabricated and covered with an antireflection coating made up of alternating layers of TiO<sub>2</sub> and SiO<sub>2</sub>. The optical properties of these materials were characterized at room temperature using ellipsometric measurements. The optimal thickness of the dielectric layers for maximum absorbance in the TES is determined using a python library described in [26].

On the right of fig. 5, simulation results demonstrate the potential improvement in TES absorption at 930 nm, comparing the absorption of the bare TES with that of the optimized TES. This design can be optimized for different TES materials and wavelengths. In fact, for the QHaloS experiment, simulations show that the dielectric thickness can be optimized to achieve an absorption of over 90% for a TiAu TES.

## 7. – Conclusion

In conclusion, this paper shows that transition-edge sensors are versatile and powerful detectors for a wide range of applications from quantum optics to particle physics. For the SEQUME project TESs are being optimized for two different wavelengths and provide high detection rates, making them ideal for traceable characterisation of single photon sources. Furthermore, in the PTOLEMY project we are working to achieve extremely precise energy resolution, necessary for the detection of relic neutrinos, opening up the possibility of obtaining a picture of the early universe. Finally, I showed that with the QHaloS experiment TESs can play a role in the dark matter search in particular dark

photons, enabling the exploration of previously untapped parameter space in a lab-scale environment. These results highlight the potential of TESs detectors and point towards possibilities for future research and innovation.

\* \* \*

The author would like to thank Mauro Rajetri, Eugenio Monticone, and Hobey Garrone for their support in the everyday work at INRiM. The author would like to thank the partners of the PTOLEMY project for their valuable collaboration and support, including the Grant (62313) from the John Templeton Foundation. The author also extend his appreciation to the partners of the SEQUME project and PTB for the opportunity to join the Guest research program. Additionally, the author would like to acknowledge the collaborative efforts of Laura Manenti, the PI of the QhaloS experiment, and Isaac Sarnoff. The author would like to thank Danilo Serazio, QR laboratory and Nanofacility Piemonte for the valuable technical support.

## REFERENCES

- [1] IRWIN K. D. and HILTON G. C., *Transition-edge sensors*, in *Cryogenic particle detection* (Springer) 2005, pp. 63–150.
- [2] ULLOM J. N. and BENNETT D. A., *Supercond. Sci. Technol.*, **28** (2015) 084003.
- [3] CABRERA B., CLARKE R., COLLING P., MILLER A., NAM S. and ROMANI R., *Appl. Phys. Lett.*, **73** (1998) 735.
- [4] IRWIN K., *Appl. Phys. Lett.*, **66** (1995) 1998.
- [5] CUNNINGHAM M., ULLOM J., MIYAZAKI T., LABOV S., CLARKE J., LANTING T., LEE A. T., RICHARDS P., YOON J. and SPIELER H., *Appl. Phys. Lett.*, **81** (2002) 159.
- [6] RAJTERI M., TARALLI E., PORTESI C., MONTICONE E. and BEYER J., *Metrologia*, **46** (2009) S283.
- [7] FUKUDA D., FUJII G., NUMATA T., AMEMIYA K., YOSHIZAWA A., TSUCHIDA H., FUJINO H., ISHII H., ITATANI T., INOUE S. *et al.*, *Opt. Express*, **19** (2011) 870.
- [8] MILLER A. J., NAM S. W., MARTINIS J. M. and SERGIENKO A. V., *Appl. Phys. Lett.*, **83** (2003) 791.
- [9] GERRITS T., LITA A., CALKINS B. and NAM S. W., *Superconducting Transition Edge Sensors for Quantum Optics*, in *Superconducting Devices in Quantum Optics*, edited by HADFIELD R. and JOHANSSON G. (Springer, Cham) 2016, pp. 31–60.
- [10] KÜCK S., LÓPEZ M., HOFER H., GEORGIEVA H., CHRISTINCK J., RODIEK B., PORROVECCHIO G., ŠMID M., GÖTZINGER S., BECHER C. *et al.*, *Appl. Phys. B*, **128** (2022) 28.
- [11] <https://sequme.cmi.cz/>.
- [12] BARACCHINI E., BETTI M., BIASOTTI M., BOSCA A., CALLE F., CARABE-LOPEZ J., CAVOTO G., CHANG C., COCCO A., COLIJN A. *et al.*, arXiv preprint, arXiv:1808.01892 (2018).
- [13] BETTI M., BIASOTTI M., BOSCA A., CALLE F., CANCI N., CAVOTO G., CHANG C., COCCO A., COLIJN A. *et al.*, *J. Cosmol. Astropart. Phys.*, **2019** (2019) 047.
- [14] MANENTI L., MISHRA U., BRUNO G., ROBERTS H., OIKONOMOU P., PASRICHA R., SARNOFF I., WESTON J., ARNEODO F., DI GIOVANNI A. *et al.*, *Phys. Rev. D*, **105** (2022) 052010.
- [15] DRUNG D., ABMANN C., BEYER J., KIRSTE A., PETERS M., RUEDE F. and SCHURIG T., *IEEE Trans. Appl. Supercond.*, **17** (2007) 699.
- [16] GARRONE H., PEPE C., REINERI A., MONTICONE E., FILIPPO R. and RAJTERI M., *IEEE Trans. Appl. Supercond.*, **32** (2022) 1.
- [17] MARTINIS J. M., HILTON G. C., IRWIN K. D. and WOLLMAN D. A., *Nucl. Instrum. Methods Phys. Res. A*, **444** (2000) 23.



- [18] LOLLI L., TARALLI E., RAJTERI M., NUMATA T. and FUKUDA D., *IEEE Trans. Appl. Supercond.*, **23** (2013) 2100904.
- [19] KOBAYASHI R., HATTORI K., INOUE S. and FUKUDA D., *IEEE Trans. Appl. Supercond.*, **29** (2019) 1.
- [20] IRWIN K. D., HILTON G. C., WOLLMAN D. A. and MARTINIS J. M., *J. Appl. Phys.*, **83** (1998) 3978.
- [21] LOLLI L., TARALLI E., PORTESI C., MONTICONE E. and RAJTERI M., *Appl. Phys. Lett.*, **103** (2013) 041107.
- [22] HATTORI K., KONNO T., MIURA Y., TAKASU S. and FUKUDA D., *Supercond. Sci. Technol.*, **35** (2022) 095002.
- [23] RAJTERI M., BIASOTTI M., FAVERZANI M., FERRI E., FILIPPO R., GATTI F., GIACHERO A., MONTICONE E., NUCCIOTTI A. and PUIU A., *J. Low Temp. Phys.*, **199** (2020) 138.
- [24] FABBRICHESI M., GABRIELLI E. and LANFRANCHI G., *The Physics of the Dark Photon: A Primer* (Springer) 2021.
- [25] RAJTERI M., RASTELLO M. L. and MONTICONE E., *Nucl. Instrum. Methods Phys. Res. A*, **444** (2000) 461.
- [26] BYRNES S. J., arXiv preprint, arXiv:1603.02720 (2016).